

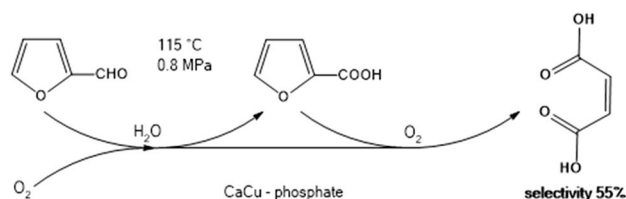
# Aqueous-Phase Oxidation of Furfural to Maleic Acid Catalyzed by Copper Phosphate Catalysts

Tomáš Soták<sup>1</sup>  · Milan Hronec<sup>1</sup> · Miroslav Gál<sup>2</sup> · Edmund Dobročka<sup>3</sup> · Jaroslava Škriniarová<sup>4</sup>

Received: 19 July 2017 / Accepted: 13 September 2017  
© Springer Science+Business Media, LLC 2017

**Abstract** This work describes catalytic aqueous-phase oxidation of furfural to maleic acid. The heterogeneous Cu-phosphate catalysts were prepared by coprecipitation method at different atomic ratios of precursors and characterized by various techniques. The CaCu-phosphate catalyst showed the best catalytic performance. Using this catalyst under reaction conditions (115 °C and 0.8 MPa of O<sub>2</sub>) 37.3 mol% yield and 54.8% selectivity of maleic acid were achieved. This catalyst can be recycled more than four times producing practically the same selectivity as fresh one by 13% decrease in furfural conversion. The proposed mechanism involves furoic acid as an intermediate in the formation of maleic acid.

## Graphical Abstract



**Keywords** Furfural · Oxidation · Metal pyrophosphates · Maleic acid · Furoic acid

## 1 Introduction

The major challenge today is to convert biomass as feedstock into useful chemicals for the chemical and pharmaceutical industries in an economically viable fashion. Furfural is a renewable resource coming from agricultural byproducts, hemicelluloses, by dehydration in acidic media. Currently it is used as a solvent and as a platform compound for synthesis of variety of chemicals and engine fuels [1, 2]. Selective oxidation of biomass-based furfural to maleic acid or anhydride which is currently manufactured from benzene and/or butane is an alternative route to the on-going fossil based processes. Maleic acid is applied in the synthesis of plasticizers, copolymers, resins, surface coatings, lubricants and agricultural chemicals.

In literature is described oxidation of furfural in both vapor and liquid phases using various types of metal catalysts [3, 4]. In spite of oxidation of furfural in vapor phase where the main products are maleic anhydride and carbon dioxide, the oxidation in the liquid phase, depending on the catalyst and solvent, can produce 2-furancarboxylic acid (furoic acid) eventually its esters or furan-ring opening

**Electronic Supplementary Material** The online version of this article (doi:10.1007/s10562-017-2191-5) contains supplementary material, which is available to authorized users.

✉ Tomáš Soták  
tomas.sotak@stuba.sk

✉ Milan Hronec  
milan.hronec@stuba.sk

<sup>1</sup> Department of Organic Technology, Catalysis and Petroleum Chemistry, Slovak University of Technology, Radlinského 9, 812 37 Bratislava, Slovakia

<sup>2</sup> Department of Inorganic Technology, Slovak University of Technology, Radlinského 9, 812 37 Bratislava, Slovakia

<sup>3</sup> Institute of Electrical Engineering, Slovak Academy of Sciences, Dúbravská cesta 9, 845 41 Bratislava, Slovakia

<sup>4</sup> Institute of Electronics and Photonics, Slovak University of Technology, Ilkovičova 3, 812 19 Bratislava, Slovakia

product maleic acid. Generally, the main drawback of catalyzed aerobic oxidations of organic substrates is low selectivity. Traditionally, oxidations conducted in the liquid-phase have been catalyzed by dissolved salts of redox-active metals. Several metallic catalysts were studied for the oxidation of furfural or its derivatives, but usually with limited selectivity for desired oxidized products [4, 5]. The major problem of low selectivity is mostly connected with polymerization of furfural to resins under oxidative conditions. Yin et al. [6] using combination of copper nitrate with phosphomolybdic acid obtained 49.2% yield of maleic acid with 51.7% selectivity. Kinetics of oxidation of furfural to 2-furancarboxylic acid using alum-impregnated activated alumina studied Kumar et al. [7]. The more challenging results were achieved recently using heterogeneous Au/ZrO<sub>2</sub> catalyst; however, in the oxidative esterification of furfural with CH<sub>3</sub>OH [8]. This catalyst is very active and selective to methylfuroate (after 90 min both conversion and selectivity are complete) and no acetal formation was observed. Metal-free oxidative synthesis of succinic acid from furfural and its homologues in the presence of hydrogen peroxide described Erbitani et al. [9, 10]. Maximum succinic acid yield and H<sub>2</sub>O<sub>2</sub> utilization efficiency of 74 and 85%, respectively, were achieved using Amberlyst-15 as a reusable solid acid catalyst. Du et al. [11] studied ring-opening oxidation of 4-hydroxymethyl furfural with molecular oxygen in acetonitrile. In the presence of homogeneous VO(acac)<sub>2</sub> catalyst maleic acid in about 52% yield was obtained. Li et al. [12] studied binary Mo–V metal oxides as catalysts for the selective oxidation of furfural to the mixture of maleic acid and maleic anhydride in acetic acid as a solvent. Under optimal conditions over the Mo<sub>4</sub>VO<sub>14</sub> catalyst up to 65% yield of maleic anhydride and maleic acid (in the ratio 1.8:1) was achieved. The recent development on maleic acid synthesis from biomass-derived chemicals over homogeneous or heterogeneous catalysts was presented lately in the review paper [13].

In the present contribution, we have investigated the oxidation of furfural to maleic acid in water as a solvent. The main objective was to study the influence of various heterogeneous copper-phosphate catalysts and reaction conditions on the activity and selectivity of the formation of maleic acid. Recycling experiments were conducted to check the stability of selected heterogeneous catalysts during oxidation reaction.

## 2 Experimental

### 2.1 Materials

Furfural (98%), maleic acid (99%), furoic acid (98%), and other chemicals were purchased from Sigma-Aldrich.

Furfural was purified by vacuum distillation and stored at –15 °C.

### 2.2 Catalyst Preparation and Characterization

The copper–phosphate catalysts were prepared by precipitation of the copper nitrate solution with an ammonium monohydrate orthophosphate solution at different molar ratios of Cu/P precursors. The hydrogen phosphate solution was added dropwise to the metal nitrate solution while stirring vigorously at ambient temperature. The precipitate was stirred for 3 h, then filtered and excessively washed with deionized water to extract the residues of the precursors. The mixed copper–metal (Mg, Ca, Sr, Ba)–phosphate catalysts were prepared accordingly, mixing corresponding metal-copper nitrate solutions at different atomic ratios of M/Cu/P precursors. All the catalysts prior to catalytic tests were calcined at 600 °C in air flow for 5 h, with a heating rate of 10 °C min<sup>–1</sup>. The Cu/P molar ratios of prepared Cu-phosphate catalysts are summarized in Table S1 (see Supplementary Data).

### 2.3 Apparatus and Oxidation Tests

Oxidation reactions were carried out in 10 mL stainless steel autoclaves lined with glass and equipped with valve. The autoclave was charged with furfural, water and catalyst and after closing pressurized with oxygen (usually 0.8 MPa). The reactors were heated in oil bath and the reaction mixture was magnetically stirred. After reaction, the solid part containing the catalyst was separated from the reaction mixture by centrifugation. In the catalyst recycle study the reaction mixture was centrifuged at 4500 rpm for 15 min and after centrifuging the catalyst was located on the bottom of the vessel as a solid phase. Then very carefully was removed about 95% of the supernatant liquid and to the settled down solid phase was added ca. 5 mL of deionized water. After mixing (ca. 5 min) and subsequent centrifugation the supernatant liquid was again removed. This procedure was repeated twice to ensure that all water soluble reaction products were recovered from the catalyst (Table 1).

### 2.4 Analysis

The liquid samples were analyzed by high performance liquid chromatography equipped with UV and RID detectors, using a HPX-87H column and 5 mmol L<sup>–1</sup> sulfuric acid aqueous solution as the mobile phase with 0.65 mL min<sup>–1</sup> flow rate. In selected samples the contents of maleic acid was checked also by gravimetric analysis of the washed and dried solid formed by precipitation with aqueous solution of barium hydroxide. In some samples was determined by gas chromatography (Shimadzu GC 2014 with TCD) the

**Table 1** Acidity of catalysts prepared at different molar ratios of precursors

Catalyst	Cu/P ratio	Ca/Cu ratio	Ca:Cu:P ratio	$a_T$ (mmol $g^{-1}_{CAT}$ )
$Cu_2P_2O_7$	0.5	–	–	0.090
	1.0	–	–	0.080
	1.5	–	–	0.075
	2.0	–	–	0.065
$CaCuP_2O_7$	0.5	–	–	0.090
	0.5	0.5	0.5:1:2	0.050
	0.5	1.0	1:1:2	0.030
	0.5	1.5	1.5:1:2	0.025

$a_T$  Total acidity (mmol  $g^{-1}_{CAT}$ )

concentration of carbon oxides in the gas phase. The identification of main products was done by NMR spectroscopy. The product yield was calculated by

$$Y = [(\text{product}_{\text{detected}}/\text{substrate}_{\text{input}}) \times 100]$$

## 2.5 Catalyst Characterization

The BET surface area of the samples was determined by nitrogen adsorption at 77 K after activation of the sample in vacuum at 300 °C for 2 h. Powder X-ray diffraction (XRD) patterns were acquired on a Bruker AX S D8 diffractometer using  $CuK\alpha$  radiation. Crystalline phases were identified by a comparison with the PDF file. The morphology of the metal phosphate catalysts was followed by SEM analysis using a JEOL JSM-7500F microscope. Temperature programmed reduction was carried out using a Micromeritics Pulse Chemisorb 2700 apparatus. The acidity of catalysts was measured by amine titration method. The sample of solid catalyst (0.2 g) was suspended in 25 mL of water using a magnetic stirrer and agitated for 30 min. The suspension was titrated with 0.1 M solution of ethylamine dissolved in water. During the titration procedure, the pH value of the solution was continuously measured. On the base of ethylamine consumption was calculated the acidity in terms of mmol  $g^{-1}$  catalyst. Abrasive linear sweep voltammetry (AbLSV) using a carbon paste electrode (CPE) as a working electrode and a platinum mesh as a counter electrode was performed. The solid catalyst samples were mechanically deposited over the working electrode surface. The voltammetric patterns curves were recorded using PGSTAT 302N (Metrohm, Switzerland) in an argon-purged phosphate buffer (pH 7.4). Saturated calomel electrode (SCE) was served as a reference electrode (RE). The measurements were carried out at  $25 \pm 1$  °C for each catalyst and were repeated at least three times. Freshly cut and polished electrode surface was used; and the measurements in the potential range from  $-0.4$  V versus RE to  $0.4$  V versus RE with potential sweep

**Table 2** Electrode potentials and Cu(I) peak areas of monometallic  $Cu_2P_2O_7$  and bimetallic M-Cu-phosphates prepared at different molar ratios

M:Cu:P molar ratio	Catalyst	Electrode potential versus RE*/V	Peak area $\times 10^{-9}$ (Coulomb)
1:1	$Cu_2P_2O_7$	$-0.042 \pm 0.021$	$0.5 \pm 0.1$
1:1:2	$MgCuP_2O_7$	$-0.027 \pm 0.018$	$8.0 \pm 1.1$
1:1:2	$CaCuP_2O_7$	$-0.038 \pm 0.012$	$14.7 \pm 2.3$
1:1:2	$SrCuP_2O_7$	$-0.055 \pm 0.014$	$5.2 \pm 0.8$
1:1:2	$BaCuP_2O_7$	$-0.068 \pm 0.008$	$1.1 \pm 0.3$
0.5:1:2	$CaCuP_2O_7$	$-0.032 \pm 0.012$	$6.4 \pm 1.2$
1:1:2	$CaCuP_2O_7$	$-0.038 \pm 0.012$	$14.7 \pm 2.3$
1.5:1:2	$CaCuP_2O_7$	No oxidation peak	

\*RE Reference electrode (saturated calomel electrode)

rate of 3 mV/s were performed. The obtained results are summarized in Table 2.

## 3 Results

### 3.1 XRD Characterization

Copper phosphate formed after precipitation of copper nitrate solution with an ammonium monohydrate orthophosphate solution is known to transform to copper pyrophosphate,  $Cu_2P_2O_7$  at the temperature of calcination of 600 °C [14]. The XRD patterns of calcined samples of copper phosphates prepared by precipitation of copper nitrate solution at the atomic ratios of Cu:P=0.5 and 1.25 confirmed (Fig. 1) that both samples were well crystallized. The sample prepared at the ratio Cu:P=0.5 contains a very pure  $Cu_2P_2O_7$  phase (PDF No. 00-044-0182) with a particle size  $23.2 \pm 0.2$  nm, but in the sample prepared at the ratio Cu:P=1.25 a very small amount of  $Cu(HPO_4)(H_2O)$  (PDF No. 01-083-1857) and  $CuHPO_3(H_2O)_2$  (PDF No. 01-072-1367) phases was present. The presence of the peak patterns corresponding to the precursor  $Cu_3(PO_4)_2 \cdot 3H_2O$  (Fig. 1a, PDF No. 00-022-0548) was not registered in these samples.

The parent Ca–Cu phosphate represents a mixed phase system. As being a co-precipitate, one can expect various separated phosphates of copper and calcium, and bimetallic phosphates. The calcination temperature of the precipitate should favor the preference of pyrophosphates over orthophosphates or hydrogen phosphates in the resulting material [15, 16]. In the binary Ca–Cu phosphate sample prepared at the atomic ratios of Ca/Cu/P precursors 1:1:2 monometallic copper pyrophosphate  $Cu_2P_2O_7$  and calcium phosphate  $Ca_3(PO_4)_2$  (PDF No. 00-029-0359) were found as dominant phases in the diffraction region below 37° (Fig. 2). In this sample are present peak patterns corresponding to the  $CaCuP_2O_7$  (PDF No. 01-080-0706) and

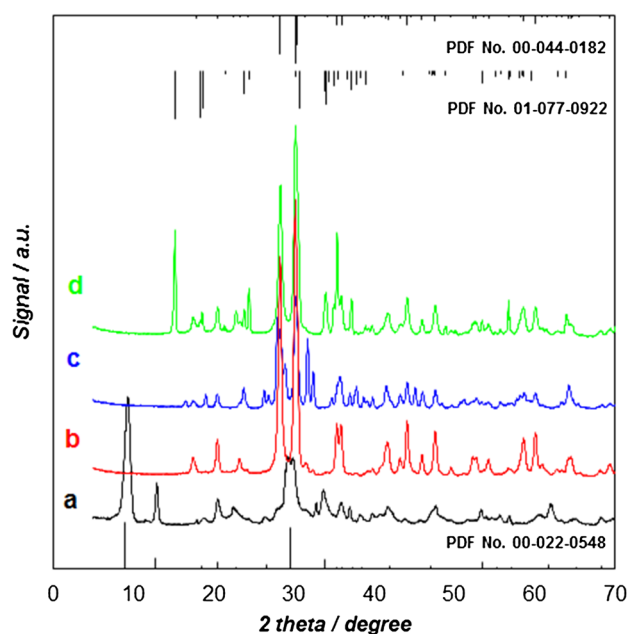


**Fig. 1** XRD patterns of  $\text{Cu}_2\text{P}_2\text{O}_7$  samples prepared at molar ratio Cu/P *a* 0.5; *b* 1.0; *c* 1.25; *d* sample (*c*) after catalytic test; phases of  $\text{Cu}_3(\text{PO}_4)_2 \cdot 3\text{H}_2\text{O}$  (PDF No. 00-022-0548),  $\text{Cu}_2\text{P}_2\text{O}_7$  (PDF No. 00-044-0182) and  $\text{Cu}_2(\text{OH})\text{PO}_4$  (PDF No. 01-077-0922)

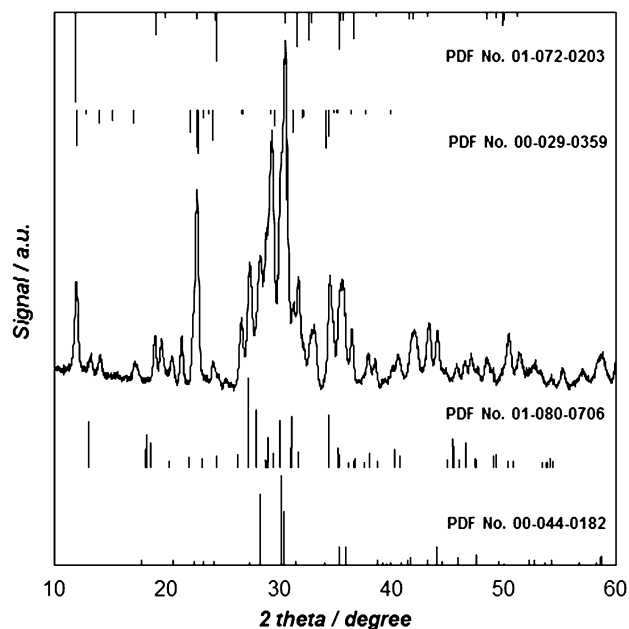


**Fig. 2** Typical XRD image of mixed Ca–Cu-phosphate prepared by calcination of precipitate synthesized at molar ratios Ca:Cu:P = 1:1:2: phases of  $\text{Cu}_2\text{P}_2\text{O}_7$  (PDF No. 00-044-0182),  $\text{CaCuP}_2\text{O}_7$  (PDF No. 01-080-0706),  $\text{Ca}_3(\text{PO}_4)_2$  (PDF No. 00-029-0359) and  $\text{Ca}_3\text{Cu}_3(\text{PO}_4)_4$  (PDF No. 01-072-0203)

$\text{Ca}_3\text{Cu}_3(\text{PO}_4)_4$  (PDF No. 01-072-0203) phases. The presence of  $\text{Cu}_3(\text{PO}_4)_2 \cdot 3\text{H}_2\text{O}$  phase (PDF No. 00-022-0548) in this

sample was not confirmed. However, the small shift of the crystallographic parameters indicates that a partial mutual substitution of Cu and Ca occurred in these phases, leading to a deformation of the crystalline structures. This cation exchange takes place probably during the calcination. A very complex XRD pattern of sample of Ca–Cu phosphate shows, that in the mixed Ca–Cu phosphate various purely defined structures can be formed [17].

### 3.2 SEM Characterization

The morphology of the monometallic  $\text{Cu}_2\text{P}_2\text{O}_7$  catalysts can be significantly altered by changing the method of their preparation. A precipitation of copper nitrate by various amounts of ammonium hydrogen phosphate followed by calcination at 600 °C resulted in different structures with relatively large crystals, or in poorer crystalline. Figure 3 shows typical SEM images of calcined samples synthesized at various conditions. The samples prepared at the atomic ratios of Cu:P = 0.5 and 1.0 possessed the agglomeration of micron sized irregular particles with rather crystalline structure. The size of crystals was above 1  $\mu\text{m}$  (Fig. 3a, b, e, f). However, the sample prepared at higher ratio (Cu:P = 1.25) displays SEM images of porous spheres structures with many nanopores (Fig. 3c, g). This phenomenon can be also seen in Fig. 3d, h for the sample of mixed Ca–Cu phosphate; we also find that there are many nanopores and the morphology of the sample has the porous spheres structure. The specific surface areas of the phosphate catalysts correspond with their morphology observed by SEM. All samples had a specific surface area smaller than 10  $\text{m}^2 \text{g}^{-1}$ .

### 3.3 TPR Characterization

TPR measurements were performed to investigate the reducibility of both copper-phosphate and mixed Ca–Cu-phosphate samples prepared at different molar ratios of the precursors and calcined at 600 °C (Fig. 4). The copper-phosphate samples displayed two reduction peaks corresponding to reduction of Cu(II) and Cu(I) species at lower and higher temperatures. As is seen from Fig. 4a–c with increasing Cu/P ratio during samples preparation both reduction peaks are shifted to higher temperatures. As the SEM images shows the shift of reduction peaks can be ascribed to different morphology of these samples. Similar dependence of reducibility temperature of copper species on the molar ratios of the precursors was observed also for the mixed Ca–Cu-phosphate samples (Fig. 4d–f). Moreover, in comparison to Cu-phosphate samples in mixed Ca–Cu-phosphates the reduction temperatures of both Cu(II) and Cu(I) species were more than 60 °C higher.

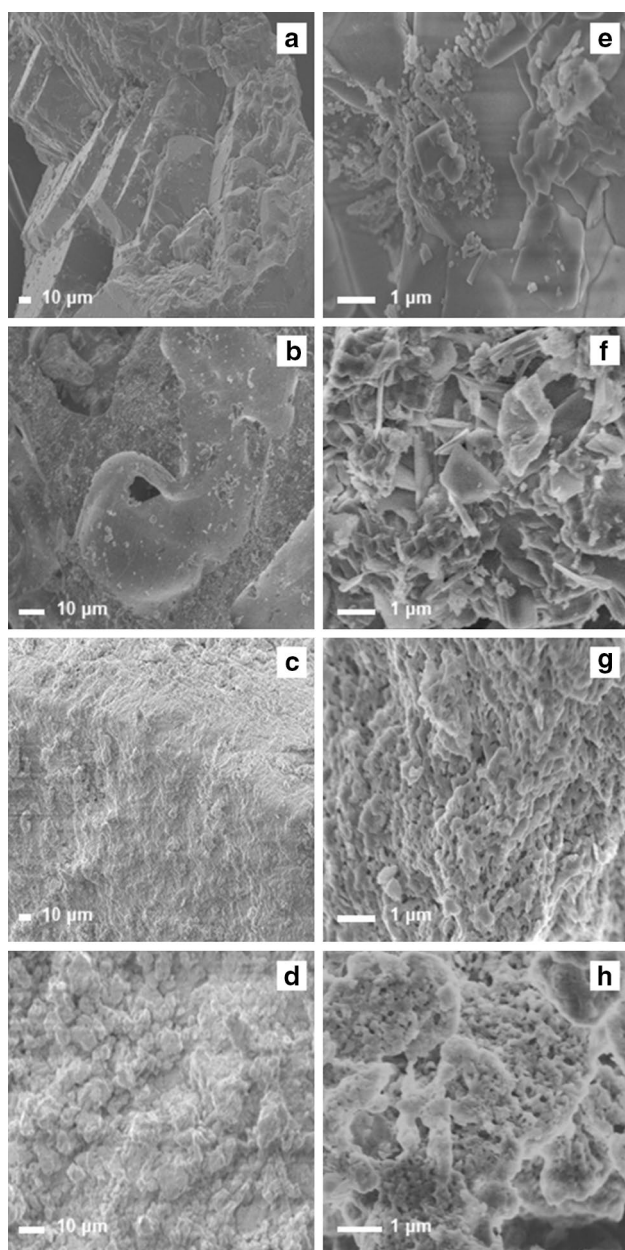


**Fig. 3** SEM images of  $\text{Cu}_2\text{P}_2\text{O}_7$  prepared at Cu:P ratios (a, e) 0.5; (b, f) 1.0; (c, g) 1.25 and (d, h) mixed Ca–Cu-phosphate synthesized at molar ratios Ca:Cu:P=1:1:2 and their magnified views

### 3.4 Acidity of Catalysts

Table 1 shows acidity of samples synthesized at various molar ratios of copper and phosphate precursors and calcined at 600 °C. As is evident from results the total acidity of  $\text{Cu}_2\text{P}_2\text{O}_7$  samples decreases from 0.090 to 0.065  $\text{mmol g}^{-1}_{\text{CAT}}$  by increasing Cu/P atomic ratio from 0.5 to 2.0. Stronger decrease in acidity is observed in mixed Ca–Cu-phosphates. The presence of calcium at the atomic ratio Ca/Cu=0.5 decreases the acidity of sample from 0.090

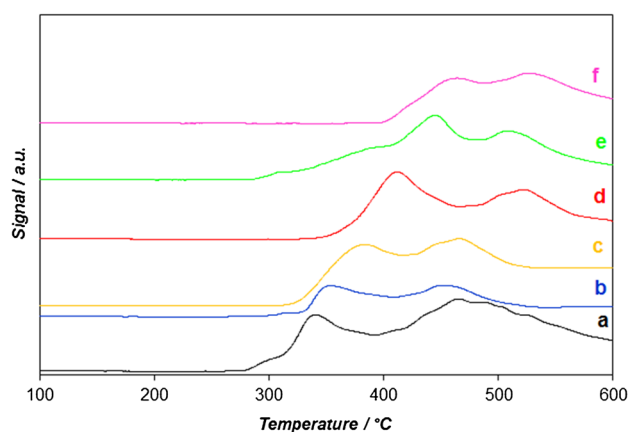


**Fig. 4** TPR profiles of  $\text{Cu}_2\text{P}_2\text{O}_7$  and  $\text{CaCuP}_2\text{O}_7$  catalysts with different Cu/P and Ca/Cu ratios: (a)  $\text{Cu}_2\text{P}_2\text{O}_7$  (Cu/P=0.5); (b)  $\text{Cu}_2\text{P}_2\text{O}_7$  (Cu/P=1.25); (c)  $\text{Cu}_2\text{P}_2\text{O}_7$  (Cu/P=2); (d)  $\text{CaCuP}_2\text{O}_7$  (Ca/Cu=0.5); (e)  $\text{CaCuP}_2\text{O}_7$  (Ca/Cu=1); (f)  $\text{CaCuP}_2\text{O}_7$  (Ca/Cu=1.5)

to 0.050  $\text{mmol g}^{-1}_{\text{CAT}}$  and in the sample at the ratio Ca/Cu = 1.5 to 0.025  $\text{mmol g}^{-1}_{\text{CAT}}$ . The drop of acidity with increasing Cu/P and Ca/Cu atomic ratios in the samples was expected since copper and calcium possess properties of bases.

### 3.5 Catalytic Tests

Catalytic oxidations of furfural using prepared copper-phosphate type catalysts were carried out at 115 °C and 0.8 MPa of oxygen pressure in aqueous solution. The major product formed in oxidation was maleic acid present in an aqueous phase and carbon dioxide in the gas phase. In most samples was identified by HPLC in liquid phase also presence of small amounts of furoic acid.

#### 3.5.1 Preliminary Study

In our preliminary study of furfural oxidation to maleic acid, different copper based catalysts, e.g. Cu oxide, nitrate, or acetylacetonate, were tested. Using these catalysts maleic acid in the yields lower than 18% was achieved. Using the mixed Cu–Fe phosphate ( $\text{CuFeP}_2\text{O}_7$ ) [18, 19] or monometallic Fe phosphate ( $\text{Fe}_2\text{P}_2\text{O}_7$ ) catalysts the yield of maleic acid 17.1 and 15.2% were obtained. However, when monometallic  $\text{Cu}_2\text{P}_2\text{O}_7$  catalyst (Cu/P = 1.0) was used for the reaction, the yield of furfural to maleic acid was improved to 25.6%. Using this Cu-phosphate catalyst the effect of reaction temperature (Fig. S1) and the influence of oxygen pressure (Fig. S2) on the oxidation of furfural to maleic acid was studied (Supplementary Data). Over this catalyst the highest yield of maleic acid, 25.7% at 64.5% furfural conversion, was achieved at the temperature of 115 °C and 0.8 MPa of oxygen pressure. Based on these results, the research was

focused on the preparation and characterization of different copper phosphate catalysts and their testing for furfural oxidation to maleic acid under the above described reaction conditions.

### 3.5.2 Oxidation Catalyzed by $\text{Cu}_2\text{P}_2\text{O}_7$ Catalysts

The efficiencies of monometallic  $\text{Cu}_2\text{P}_2\text{O}_7$  catalysts prepared at different Cu/P atomic ratios of precursors for the oxidation of furfural to maleic acid are listed in Fig. 5. As the XRD data confirmed (Fig. 1) the samples of  $\text{Cu}_2\text{P}_2\text{O}_7$  catalysts prepared at the Cu/P atomic ratios of precursors 0.5 and 1.25 after calcinations at 600 °C display the structure of copper pyrophosphate; however, their catalytic activities are significantly different (Fig. 5). As is seen with increasing Cu/P atomic ratio increases both activity and selectivity, reaching the maximum at the ratio of 1.25 and then decreases. Among these catalysts, the  $\text{Cu}_2\text{P}_2\text{O}_7$  catalyst prepared at Cu/P atomic ratio 1.25 provides at 62.0% furfural conversion 51.3% selectivity to maleic acid and 4.5% to furoic acid. When the reaction was carried out under the same reaction conditions in the absence of metal catalyst 50.4% of furfural was converted, but maleic acid was formed only in trace amounts. It confirms that during non-catalytic oxidation the main part of furfural (about 80%) was converted to polymeric products. Since at elevated temperatures and pressures of oxygen the rate of formation of oligomers by parallel non-catalyzed reaction is enhanced, the main problem of furfural oxidation in liquid phase is how to avoid the formation of resins. As is seen from the results in Fig. 5 a significant improvement of selectivity to maleic acid is achieved in conduction of oxidation reaction in the presence of copper catalysts. The effect of these catalysts is related with the reduction of the rate of

polymerization of the reaction intermediates to resins and promoting their conversion to maleic acid.

### 3.5.3 Oxidation Catalyzed by Mixed M–Cu-phosphate catalysts

The improvement of catalytic activity and selectivity to maleic acid is achieved using mixed metal phosphate catalysts prepared by coprecipitation of the metal precursors followed by calcination at 600 °C. In Fig. 6 are the results of furfural oxidation in the presence of copper catalysts prepared in the presence of Mg, Ca, Sr and Ba salts in the atomic ratio metal/Cu = 1. Their influence on both activity and selectivity to maleic acid is in the order: Ca > Mg > Sr > Ba. Among these bimetallic catalysts, Ca–Cu phosphate provides the highest catalytic performance. In comparison to monometallic  $\text{Cu}_2\text{P}_2\text{O}_7$  catalyst prepared at the same Cu/P atomic ratio (1.0) and tested at comparable conditions the conversion of furfural and mainly selectivity to maleic acid is increasing from 64.5 and 39.8% (Fig. 5) to 68.0 and 54.8% (Fig. 6), respectively. On the other hand, the catalysts doped with Sr and Ba are less active (48.9 and 50.0% conversion, respectively), however, in comparison to monometallic  $\text{Cu}_2\text{P}_2\text{O}_7$  catalyst they are more selective to maleic acid (selectivity 43.4 and 34.7%, respectively). Comparison the activity and the selectivity of studied bimetallic copper phosphate catalysts with monometallic  $\text{Cu}_2\text{P}_2\text{O}_7$  catalyst indicates that in their presence is substantially reduced the polymerization of reaction intermediates to resins.

As was described above the highest catalytic performance for furfural oxidation to maleic acid was achieved using bimetallic Ca–Cu phosphate catalyst prepared at the atomic ratios of precursors corresponding to Ca:Cu:P = 1:1:2. During this experiment the molar ratio of furfural/Ca–Cu phosphate catalyst (calculated on Cu)

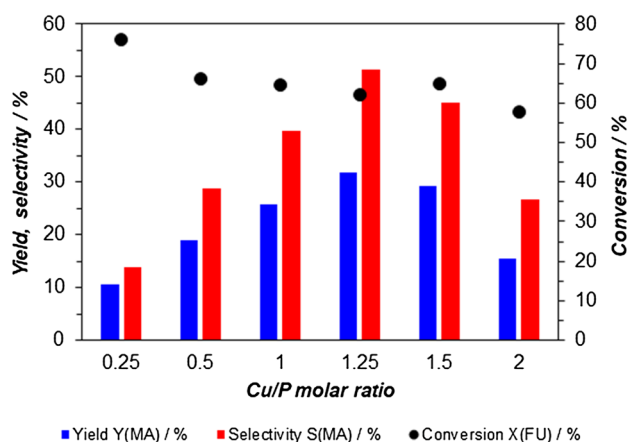


**Fig. 5** The effect of the Cu/P atomic ratio during  $\text{Cu}_2\text{P}_2\text{O}_7$  catalyst preparation on the catalyst performance. Conditions: 115 °C; 0.8 MPa oxygen; 0.250 g furfural; 5.0 mL water; 0.050 g of catalyst; reaction time 18 h

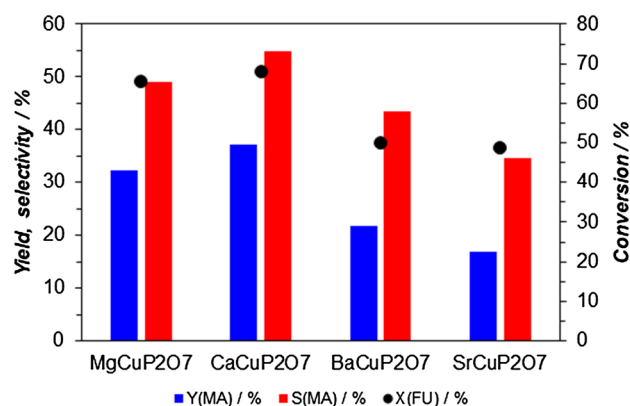


**Fig. 6** Catalytic performance of bimetallic  $\text{MCuP}_2\text{O}_7$  pyrophosphates prepared at atomic ratios Cu/P = 0.5 and M/Cu = 1; (M:Cu:P = 1:1:2). Conditions: See Fig. 5

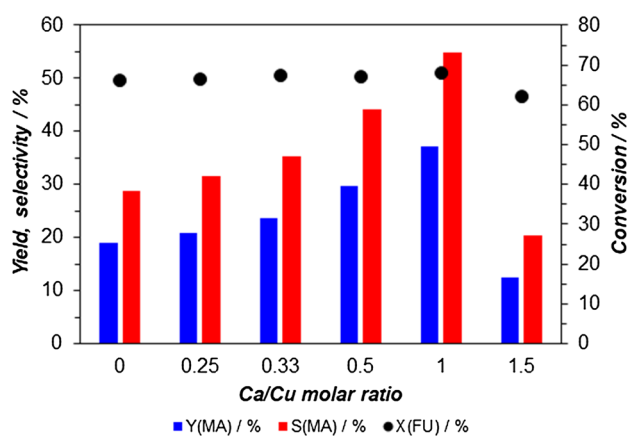


**Fig. 7** The effect of the Ca/Cu atomic ratio during preparation of  $\text{CaCuP}_2\text{O}_7$  catalyst (Cu:P=1:2) on the catalyst performance. Conditions: see Fig. 5

was 15:1. Since this bimetallic catalyst is highly efficient for furfural oxidation to maleic acid, another bimetallic catalysts with various Ca:Cu:P ratios were prepared and evaluated. In Fig. 7 is shown the influence of calcium concentration on the catalytic properties of bimetallic Ca–Cu catalysts prepared at the atomic ratio of Cu:P=0.5. From these results is clearly evident that in the range of the atomic ratios of Ca:Cu=0–1 the catalytic activity is almost the same (the conversion of furfural is about 66–68%), and only at the ratio 1.5 conversion slightly decreases (to ca. 62%). However, the presence of calcium has a highly positive effect on the selectivity of maleic acid formation. The selectivity increases from initial 28.8%, obtained with monometallic  $\text{Cu}_2\text{P}_2\text{O}_7$  catalyst, to 54.8% in the presence of bimetallic catalyst prepared at the Ca/Cu atomic ratio 1. At the ratio 1.5 the selectivity sharply decreases to about 20%. The same catalytic activity (furfural conversion) but a very strong effect of calcium on the improvement of selectivity evidently must be related with the reduction of non-selective polymerization reactions.

As was described above (Fig. 5) the selectivity of oxidation using monometallic  $\text{Cu}_2\text{P}_2\text{O}_7$  catalysts increases with increasing Cu/P atomic ratio of precursors used in the preparation step, reaching the maximum at the value of 1.25. The previous study of the influence of calcium on the catalytic performance of Ca–Cu-phosphate catalysts was followed using samples prepared at the atomic ratios Ca:Cu:P=1:1:2. To achieve better results we prepared and tested bimetallic Ca–Cu-phosphate catalysts with different Cu/P atomic ratio and having the ratio Ca:Cu=1:1. In contrary to the results depicted in Fig. 5, with increasing (Ca–Cu)/P atomic ratio decreases sharply both the catalytic activity and selectivity to maleic acid (Fig. 8). It means that in the presence of these catalysts a significant part of furfural was converted to resins.

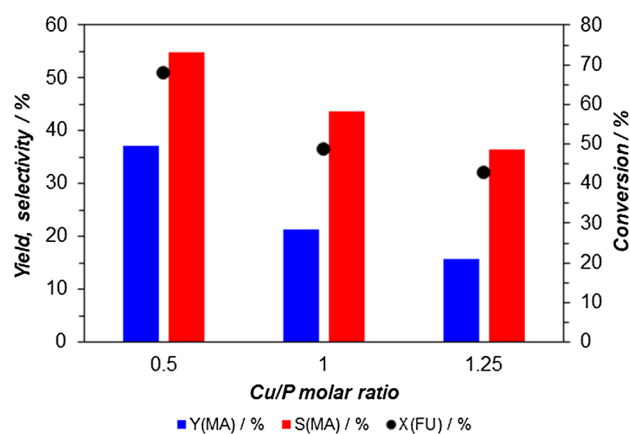


**Fig. 8** The effect of the Cu/P atomic ratio during preparation of  $\text{CaCuP}_2\text{O}_7$  catalyst (Ca:Cu=1:1) on the catalyst performance. Conditions: See Fig. 5

For better understanding of the effect of alkali earth metals in the M–Cu-phosphate structure on their catalytic performance some bimetallic phosphate catalysts using the abrasive linear sweep voltammetry (AbLSV) method were studied. As is seen from results in Table 2, for monometallic  $\text{Cu}_2\text{P}_2\text{O}_7$  catalyst a very small oxidation peak with area only  $0.5 \times 10^{-9}$  C was observed. This potential at  $-0.042 \pm 0.021$  V corresponds to the position of the oxidation peak observed for pure  $\text{Cu}_2\text{O}$ . In comparison to the monometallic Cu-phosphate, in the bimetallic M-Cu-phosphate catalysts, especially doped with calcium and magnesium, intensive oxidation peaks were registered. The position of these oxidation peaks in the catalysts is also the same as the position of the oxidation peak observed for pure  $\text{Cu}_2\text{O}$ . It suggests that in these catalysts copper in oxidation state Cu(I) is present. The most intense oxidation peak was observed for Ca–Cu-pyrophosphate catalyst (peak area  $14.7 \pm 2.3 \times 10^{-9}$  C) followed by bimetallic Mg–Cu-phosphate (peak area  $8.0 \pm 1.1 \times 10^{-9}$  C). As mentioned above (Fig. 6), using these catalysts the highest selectivity to maleic acid (54.8 and 49.0%) was achieved. For other types of bimetallic phosphates (Sr and Ba) the oxidation peak area and also their activity and selectivity to maleic acid was lower. The electrode potential of bimetallic catalysts decrease in the order: Ca > Mg > Sr > Ba. This order correlates well with changes of the yields and selectivities to maleic acid obtained using these catalysts.

### 3.5.4 Catalyst Recycling

In order to study the catalyst deactivation during the furfural oxidation, we have carried out four reaction runs using monometallic  $\text{Cu}_2\text{P}_2\text{O}_7$  catalyst and bimetallic Ca–Cu-phosphate catalyst. The catalysts were prepared at Cu/P atomic ratio 1 and bimetallic catalyst at the atomic ratios Ca:Cu:P=1:1:2.

At the end of each reaction the catalyst was filtered out, washed only with water and submitted directly to the next run. In Fig. 9 the results for both catalysts obtained after four cycles are presented. As shown in the figure despite different initial selectivity both catalysts exhibit practically the same selectivity in the first and in the fourth cycle. Catalytic activity slightly decreases, while for both catalysts this decrease exhibits the same trend; during fourth cycles conversion of furfural dropped by about 8% and about 13% for  $\text{Cu}_2\text{P}_2\text{O}_7$  and bimetallic Ca–Cu-phosphate catalyst, respectively.

The phase composition of the Cu phosphate catalyst should be changing during the catalytic tests, using oxygen as oxidizing agent. X-ray diffraction patterns of the  $\text{Cu}_2\text{P}_2\text{O}_7$  catalyst recorded after a catalytic test revealed a small modification of the catalyst in comparison with the fresh one (Fig. 1d). In the sample of recycled catalyst, the presence of peaks characteristic to the  $\text{Cu}_2(\text{OH})\text{PO}_4$  phase (PDF No. 01-077-0922), especially at  $2\theta = 15^\circ$  was registered. Despite the small amount of the formed phase these data indicate that during the catalytic test some changes of the catalyst took place. Transformation of  $\text{Cu}_2\text{P}_2\text{O}_7$  phase to copper oxides during the catalytic test was not observed. Moreover, these oxides alone are catalytically almost inactive for furfural oxidation. In order to understand the possibility that homogeneous metallic species dissolved from catalyst should be real catalyst, the filtrate of  $\text{Cu}_2\text{P}_2\text{O}_7$  catalyst treated under reaction conditions was used for the reaction. After addition of furfural and oxidation reaction comparable results with non-catalyzed oxidation of furfural were obtained (about 50% furfural conversion and less than 5% selectivity to maleic acid). Leakage of metals into solution was confirmed of less than 3 ppm in the filtrate of the reaction mixture. Therefore, the loss of activity is not only due to catalyst losses in the separation step but also by a partial dissolution of catalyst in aqueous reaction medium.

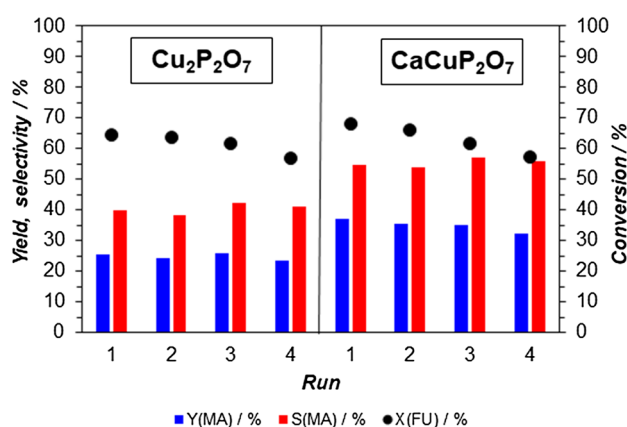


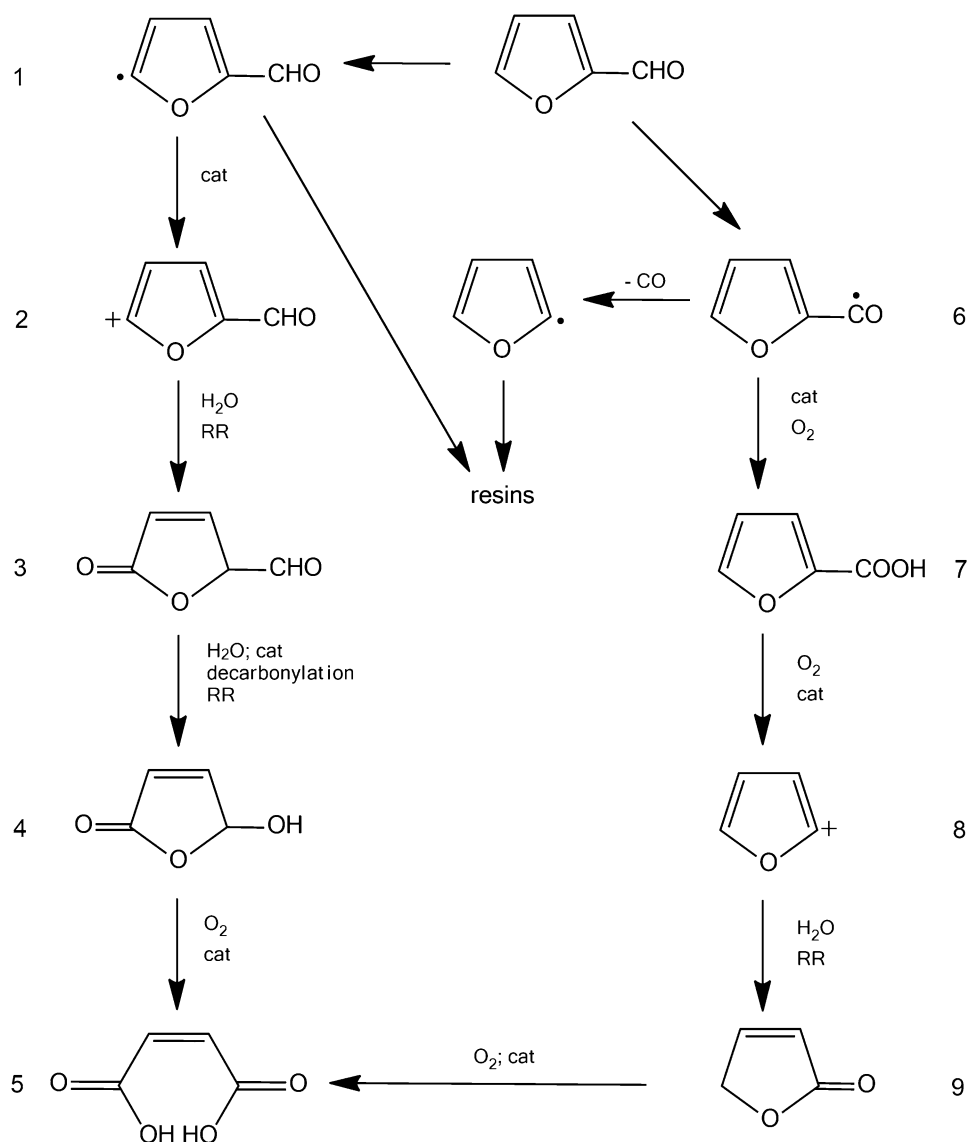
**Fig. 9** Recycling of catalysts. Conditions: See Fig. 5; catalyst  $\text{Cu}_2\text{P}_2\text{O}_7$  prepared at the ratio Cu/P=1 and catalyst  $\text{CaCu}_2\text{P}_2\text{O}_7$  prepared at the ratios Ca:Cu:P = 1:1:2

Excluded cannot be the deactivation of the catalyst by resinous by-products adsorbed on the catalyst surface since between recycling cycles the catalyst was washed only with water. Therefore, polymeric products which are insoluble in water, may remain adsorbed on the catalyst and their amount is increasing gradually with the recycling runs.

## 4 Discussion

In the literature are proposed various mechanisms for furfural oxidation using homogeneous and heterogeneous catalysts and oxygen or hydrogen peroxide as oxidation agents [3–5, 20–22]. During heterogeneously catalyzed reaction furfural molecule lies essentially flat on the surface and the  $\pi$ -electrons in the furan ring and carbonyl interacts more strongly with the surface [23, 24]. This interaction may lead to abstraction of the hydrogen atom at the 5-position of furfural or at the aldehyde group [12] and generate radicals **1,6** (Scheme 1). These radicals can attack another furfural molecule and promote the conversion of furfural to resins, or can be trapped by organic radical scavengers or some metal ions. It is well known, that copper (II) is a highly efficient trap for organic radicals to generate organic cation intermediates. Accordingly, if in the reaction system is present suitable copper catalyst the furfural radical is converted to cation intermediate **2** leading in the next steps to small oxygen containing molecules. As demonstrated in Scheme 1, in the process of furfural oxidation the electron transfer reaction generating furfural cation is crucial for competing with furfural polymerization, i.e. for achieving high selectivity of oxidation to the desired product. The rate of electron transfer reaction depends on the redox potential of copper cation (Table 2) and probably also on the geometric configuration of the sites hosting the active species (Fig. 3). As the results of furfural oxidation using monometallic  $\text{Cu}_2\text{P}_2\text{O}_7$  and bimetallic CaCu phosphate catalysts showed that the selectivity of the reaction depends on the Cu/P and Ca/Cu atomic ratio. This ratio influences the acidity (Table 1) and the morphology (Fig. 3) of catalysts and as evidenced by the  $\text{H}_2$ -TPR (Fig. 4) and voltammetry measurements (Table 2) it resulted in modified redox properties of catalysts. As was observed experimentally pure  $\text{Ca}_3(\text{PO}_4)_2$  was found to be inactive, while the activity of bimetallic Ca–Cu phosphate increased as the sample is enriched in calcium up to the atomic ratio Ca:Cu = 1 (Fig. 7). Since  $\text{Ca}_3(\text{PO}_4)_2$  alone is inactive for maleic acid formation, the role of added calcium might be attributed to the acceleration of electron transfer steps that are crucial for selective oxidation of furfural to maleic acid. Thus, adding calcium can provide the highest yield of expected product, while other alkaline earth metals may also improve the electron transfer ability of copper

**Scheme 1** A plausible mechanism for furfural oxidation to maleic acid. RR E 1,4-rearrangement; cat CuE-phosphate catalyst



catalyst (Table 2) but with less improvement than calcium (Fig. 6).

Attack of cation intermediate **2** with water, followed by 1,4-rearrangement and subsequent decarbonylation and electron transfer reaction of formed intermediate **3** generates cation intermediate which is attacked with water producing intermediate **4**. This is subsequently oxidized to maleic acid as the major product of furfural oxidation. The decarbonylation of intermediate **3** was indicated by the detection of CO and CO<sub>2</sub> in the gas mixture after reaction.

In experiments using copper phosphate catalysts was observed that beside the desired product, maleic acid, the presence of small amount of furoic acid was also registered in the reaction mixtures. It should suggest that in the initial step of furfural oxidation also hydrogen from the aldehyde group is abstracted, forming radical intermediate **6**. The intermediate **6** can decarbonylate, followed to form resins

or more likely to react with oxygen to produce furoic acid **7**. To test whether furoic acid is the final product of furfural oxidation or can be further transformed to maleic acid, we conducted a control experiment where furoic acid was separately used as a starting substrate for oxidation under the identical conditions of furfural oxidation. Using CaCu-phosphate catalyst (Ca:Cu:P = 1:1:2) 36.8 mol% yield of maleic acid from furoic acid was obtained. This yield is almost the same as was reached in the experiment with furfural (37.3 mol%, Fig. 7). Moreover, 33 mol% yield of maleic acid and 50% conversion of furoic acid was achieved already after 3 h of reaction. The rapid conversion of furoic acid to maleic acid explains why in most reaction mixtures of furfural oxidation furoic acid is present only in low concentrations. It confirms that for the current system also the pathway through furoic acid might be considered in the reaction mechanism. Probably furoic acid in the presence of copper

catalyst is decarboxylated forming cation intermediate **8** which is attacked with water, followed by 1,4-rearrangement to generate the intermediate **9**. This intermediate is further catalytically oxidized to maleic acid. Therefore, it might be assumed that in the case of studied copper phosphate catalysts a route involving furoic acid as an intermediate of furfural oxidation in water plays a role in maleic acid formation.

## 5 Conclusions

In this work, new recyclable heterogeneous catalysts have been explored to convert furfural in liquid phase to maleic acid. Several copper phosphate type catalysts were prepared by coprecipitation at different atomic ratios of precursors. The samples were calcined at 600 °C and characterized by physical–chemical methods and evaluated for the oxidation of furfural in water. Experimentally it was observed that the M/Cu/P atomic ratio of precursors in copper pyrophosphate catalysts and in mixtures with Mg, Ca, Sr, Ba metals influences the acidity and the morphology of catalysts and strongly also their catalytic performance. It is assumed that these effects are linkage to the modification of redox potential of copper cation and probably also to geometric configuration of the sites hosting the active species. Doping of copper phosphate catalyst with calcium showed the best catalytic performance for furfural oxidation to maleic acid. Under reaction temperature of 115 °C and 0.8 MPa of oxygen pressure and using CaCu-phosphate catalyst prepared at the atomic ratio of precursors Ca:Cu:P = 1:1:2, 54.8% selectivity to maleic acid can be achieved. This catalyst recovered by filtration and washed only with water could be recycled for more than four times. Despite partial leaching of metals from the catalyst to the solution the selectivity in all runs remain practically the same, and the catalytic activity (furfural conversion) after fourth cycles decreases only by about 13%. The mechanistic study of furfural oxidation leads to the assumption that in the presence of studied copper catalysts a route involving furoic acid as an intermediate plays a role in maleic acid formation.

The advantages of simple isolation and reusability of studied heterogeneous catalysts also the yields of maleic

acid provide an alternative route to the homogeneously catalyzed reaction.

**Acknowledgements** Support from the fund APVV-0297 is deeply appreciated.

## References

- Gallezot P (2012) *Chem Soc Rev* 41:1538
- Luterbacher JS, Alonso DM, Dumesic JA (2014) *Green Chem* 16:4816
- Alonso-Fagúndez N, Granados ML, Mariscal R, Ojeda M (2012) *Chem Sus Chem* 5:1984
- Lan J, Chen Z, Lin J, Yin G (2014) *Green Chem* 16:4351
- Guo H, Yin G (2011) *J Phys Chem C* 115:17516
- Shi S, Guo H, Yin G (2011) *Catal Commun* 12:731
- Kumar NS, Srivastava VC, Basu S (2013) *Indian Chem Eng* 55:153
- Pinna F, Olivo A, Trevisan V, Menegazzo F, Signoretto M, Manzoli M, Boccuzzi F (2013) *Catal Today* 203:196
- Choudhary H, Nishimura S, Erbitani K (2012) *Chem Lett* 41:409
- Choudhary H, Nishimura S, Erbitani K (2013) *Appl Catal A Gen* 458:55
- Du Z, Ma J, Wang F, Liu J, Xu J (2011) *Green Chem* 13:554
- Li X, Ho B, Zhang Y (2016) *Green Chem* 18:2976
- Wojcieszak R, Santarelli F, Paul S, Dumeignil F, Cavani F, Gonçalves RV (2015) *Sustain Chem Process* 3:9
- Induja S, Raghavan PS (2013) *Catal Commun* 33:7
- Blazy P, Samama JC (2001) *C R Acad Sci Paris* 333:271
- Özer AK, Gülaboglu MS, Bayrakceken S, Weisweiler W (2006) *Adv Powder Technol* 17:481
- Khan N, Morozov VA, Khasanov SS, Lazoryak BI (1997) *Mater Res Bull* 32:1211
- Štolcová M, Litterscheid C, Hronec M, Glaum R (2007) *Stud Surf Sci Catal* 167:37
- Polnišer R, Štolcová M, Hronec M, Mikula M (2011) *Appl Catal A Gen* 400:122
- Alba-Rubio AC, Fierro JLG, León-Reina L, Mariscal R, Dumesic JA, López Granados M (2017) *Appl Catal B* 202:269
- Alonso-Fagúndez N, Agirrezabal-Telleria I, Arias PL, Fierro JLG, Mariscal R, Granados ML (2014) *RSC Adv* 4:54960
- Li X, Lan X, Wang T (2016) *Catal Today* 276:97
- Pang SH, Medlin JW (2011) *ACS Catal* 1:1272
- Sitthisa S, Pham T, Prasomsri T, Sooknoi T, Mallinson RG, Resasco DE (2011) *J Catal* 280:17